3 EARLY WIND FORECASTING RESULTS FROM THE 1.5 KM WRF-ARW IN EXTREME SOUTHWESTERN CALIFORNIA

Ivory J. Small* and Brandt Maxwell
NOAA/NWS San Diego, CA

1. INTRODUCTION

Wind flowing into Southern California (Fig. 1) interacting with rugged terrain results in very complex weather patterns. To examine these patterns, NWS San Diego utilizes a 1.5 km nest inside of a 3.7 km local WRF-EMS ARW. It has helped in both analyzing and predicting the strength, location, onset, and cessation of a variety of phenomena driven by local wind flows. In order to examine a sampling of such phenomena, first, a sea breeze case will be explored.

Convection location, timing, and strength are also strongly modulated by wind flow in Southern California. The impacts on convection are especially significant during the warm season, when the monsoon flow from the southeast interacts with the mountain/valley flow and sea breeze flow. Convection will be investigated after the sea breeze flow case.

Downslope winds are the most expensive, and perhaps the weather phenomena that garner the most attention in southern California. Usually the Santa Ana Winds and associated fires are examined. However, in this paper, winds in the onshore direction will be analyzed. Although the focus will be at 1.5 km, some lower resolution modeling from past events will be included.

2. SEA BREEZE/UPVALLEY FLOW CASE

Figure 2, left panel, is the 15 hour forecast 1.5 km WRF-EMS ARW surface winds (green barbs), wind speed (shading), and surface observations valid at 2100 UTC 12 August 2013. The leading edge of the sea breeze front is indicated (blue line with barbs) and is seen quite well in the shading. Note the calm winds at Palm Springs (yellow METAR observation). Two hours later (at 2300 UTC 12 August 2013) the image on the right shows the sea breeze front has passed Palm Springs based on the model forecast and the observation, with gusts to 18 knots. It proved to be accurate.

*Corresponding author address: Ivory J. Small, NOAA/NWS San Diego. 11440 W. Bernardo Ct., Ste. 230, San Diego, CA 92127-1643; e-mail; ivory.small@noaa.gov

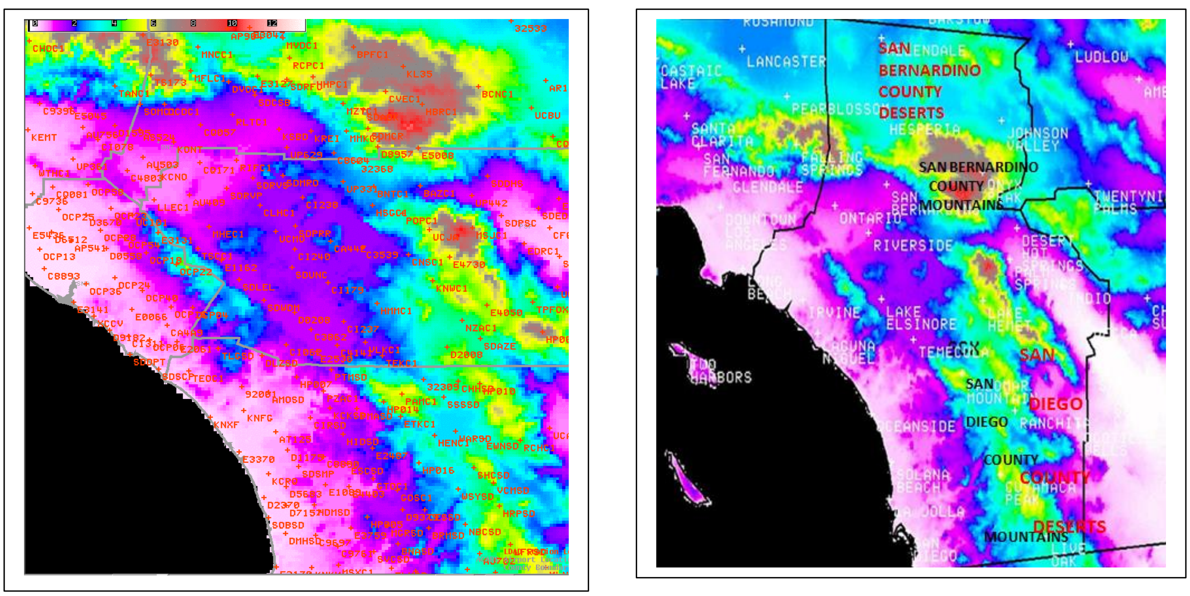

Fig. 1. Terrain map of the WFO SGX CWFA. Color coding in the legend is in thousands of feet MSL.

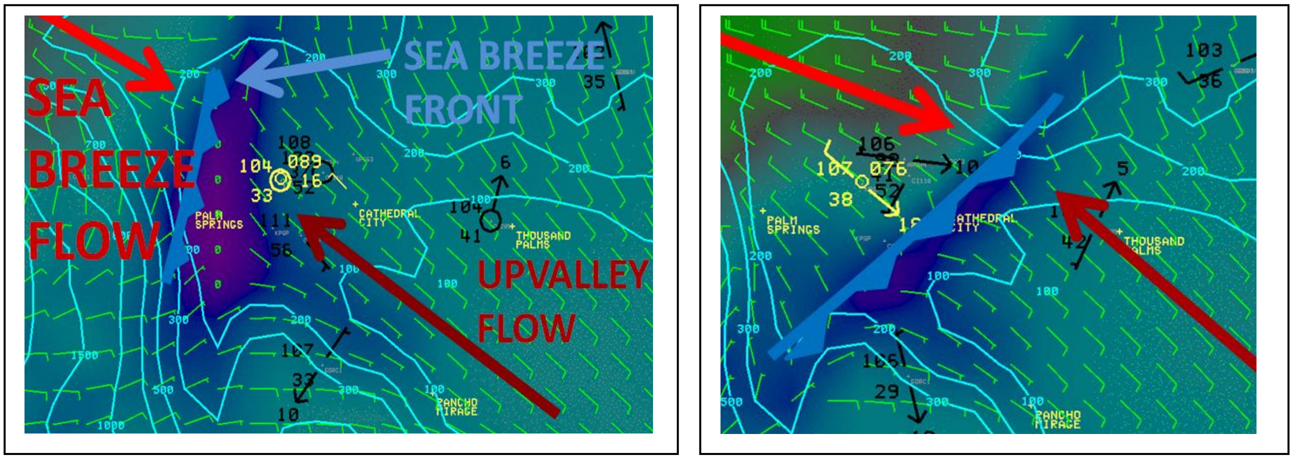

Fig. 2. The image on the left is the 15 hour forecast 1.5 km WRF-EMS ARW surface winds (green barbs), wind speed (shading), and surface observations valid at 2100 UTC 12 August 2013.
The image on the right is the 17 hour forecast 1.5 km WRF-EMS ARW surface winds (green barbs), wind speed (shading), and surface observations valid at 2300 UTC 12 August 2013.

3. CONVERGENCE PATTERNS AND THEIR EFFECT ON CONVECTION

The wind patterns help determine the convergence patterns, and the convergence patterns can effect convection location and strength [as seen in Small et al., (2000) and in figures 3 and 4]. In the following case study (a deep offshore flow case), convergence develops west of the mountain crestlines and below canyons and passes. The model reflects this pattern. East winds at the stations on the mountain crests in the satellite imagery in fig. 4 shows that the convergence is displaced to the leeside (western) slopes. Weak 700-500 mb winds also helps generate an offshore flow surface convergence pattern (surface convergence is seen via the tight gradients in the black isotachs where velocities approach zero).

The westerly sea breeze flow eventually nudges the convergence boundaries eastward during the afternoon, moving past the mountain crest. The dashed ridgeline convergence zones (fig. 3 and 4) near the mountains, (possibly beginning an event displaced off the mountain crest on the lee side), typically develops convection before the arcs downwind of the passes during very moist and unstable days, but convection may be confined to the ridgelines on relatively dry days when the LCL/LFC is high and mid-level relative humidity is rather modest. The 2200 UTC image (lower left image in fig. 4.) shows convergence lines associated with the crest of the mountains and the convergence arcs associated with the gap flow. They have been displaced to the east (typical afternoon movement). Enhanced convection (especially near Warner Springs in the north in fig. 4), develops on the convergence lines as they move eastward. The middle image in figure 3 is probably the most common when convection initiation gets underway.

The flow is parallel to most mountain ridges. (Usually south-southeasterly, so the convection sets up very close to the ridgeline). Later in the day, the onshore flow typically dominates in the north for arcs and convergence zones to drift eastward first. The eastward drift often occurs later in the south.

Sometimes, there is morning convection developing on both the desert slopes and near the coastal slopes simultaneously (with or without any convection at the ridgelines). This can occur when the air mass is very moist and unstable so the convergence forms on the easterly flow to the west of the gaps and ridgelines, and convection can be initiated via upslope flow on the desert side (often driven by persistent low level easterly winds from a gulf surge or thunderstorm outflow boundaries). Rapid fluxes of low level moisture from tropical cyclones as well as from mesoscale convective systems are notorious for this. These are typically among the most volatile days for convection, with severe weather and flash flooding not uncommon. Rapid jumps in precipitable water, up to around 1.75 inches or higher, are especially prolific generators of episodes of severe thunderstorms and flash flooding. Episodes when precipitable water peaks at around 2 inches or higher have a very high probability of flash floods and/or severe weather at some point during the episode. Upper level lows/troughs of low pressure, nearby tropical cyclones, or easterly waves help to increase the potential for severe weather and flash flooding.

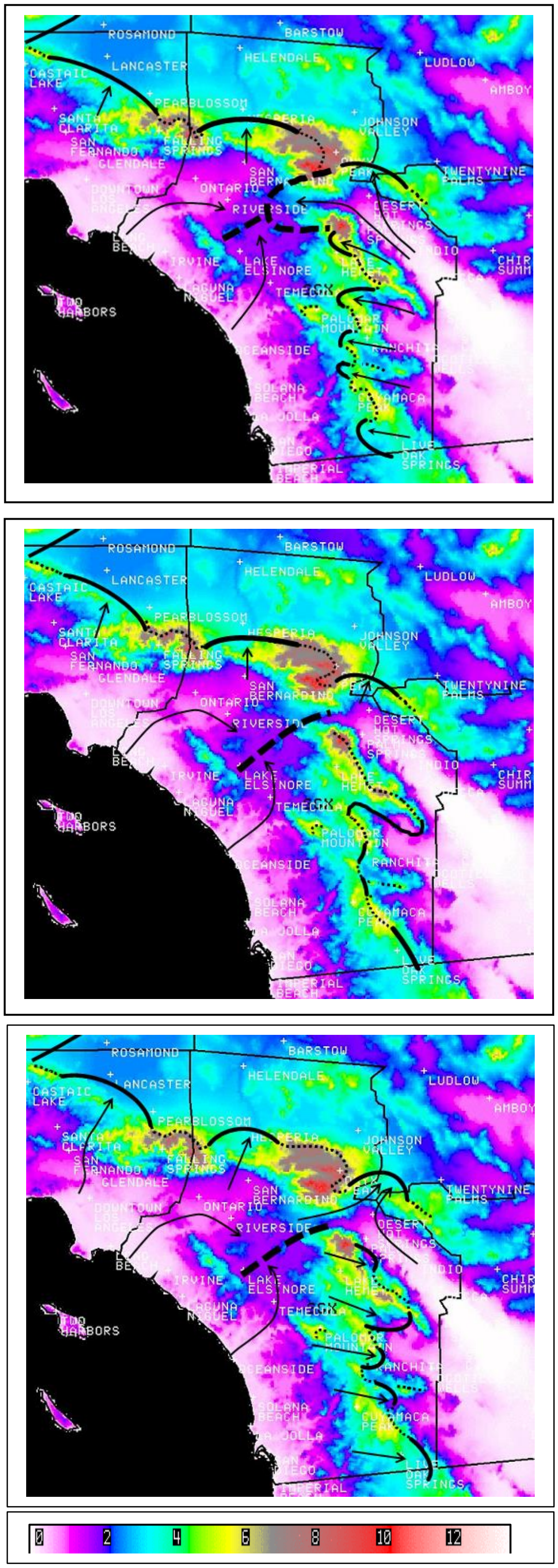

Fig. 3. Idealized schematic patterns for dominant offshore flow (top) weak cross barrier flow and/or flow that is essentially parallel to the main ridgelines (middle) and dominant onshore flow (bottom). The arrows are low-level cross-barrier (or gap) wind components. The thin dashed lines are convergence lines generated on/near mountain ridges, and the thick solid lines are convergence “arcs” downwind of passes and canyons. The thick dashed lines are the “Modified Elsinore Convergence Zone” (top) and the “Standard Elsinore Convergence Zone” (middle and bottom). The legend is in thousands of feet MSL.

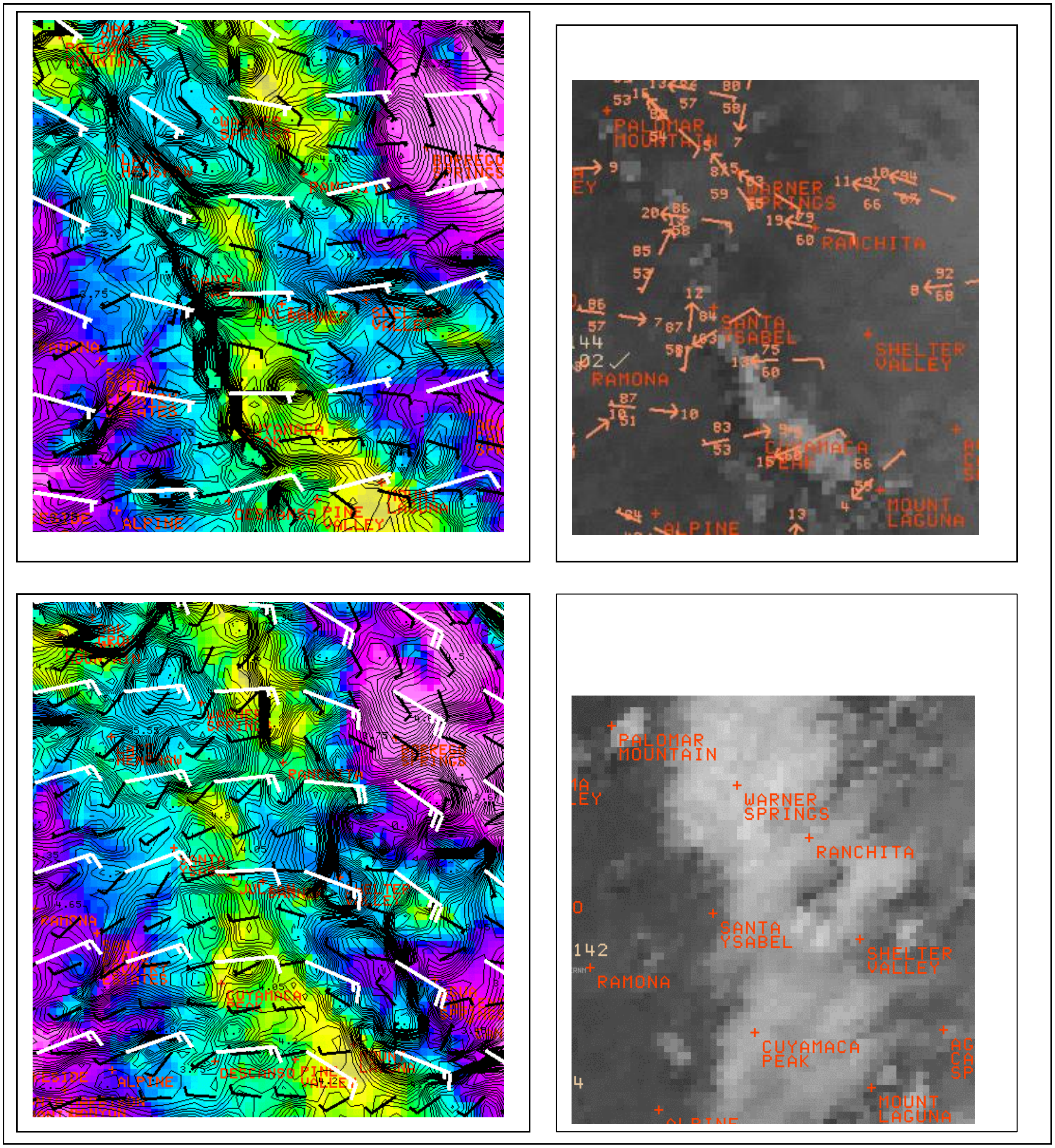

Fig. 4. The top left panel is the 30 hour 1.5 km WRF-EMS ARW surface winds (black barbs), 700-500 mb winds (white barbs), and surface wind speed (black contours) overlaid on a terrain background (shaded) valid at 1800 UTC 4 July 2014. The bottom left panel is the same, except it is the 34 hour forecast valid at 2200 UTC 4 July 2014. The visible satellite imagery and surface observations on the right corresponds to the times of the images on left (surface observations not available at 2200 UTC). Yellow areas in the terrain map are the higher mountains and the dark blues and purples are the lower elevations.

Figure 5 (imagery from 2001), even at 8 km resolution, shows several circulations. The most prominent is the circulation in the lee of the San Bernardino County Mountains, and also the circulation in the south near the Mexican Border. This convergence zone in the north, the “Lucerne Valley Cyclone” (LVC) strengthens a convergence zone between flows from either side of the San Bernardino County Mountains. It helps create very strong to severe thunderstorms and flash flooding in the area between Lucerne Valley and Big Bear Lake. These storms can propagate southeast into the highly populated Inland Empire down convergence zones like the Elsinore Convergence Zone. The 1.5 km WRF EMS-ARW should allow us to see these circulations more easily. It has been noted in the past that very strong convection develops on these circulations, especially on the northern and western flanks of these circulations. Even if there is no apparent circulation, the fact that there is unusually strong convergence there makes it a prime candidate for severe weather and flash flooding, especially on days when the LCL and LFC are low and the boundary layer moisture and dew points are unusually high.

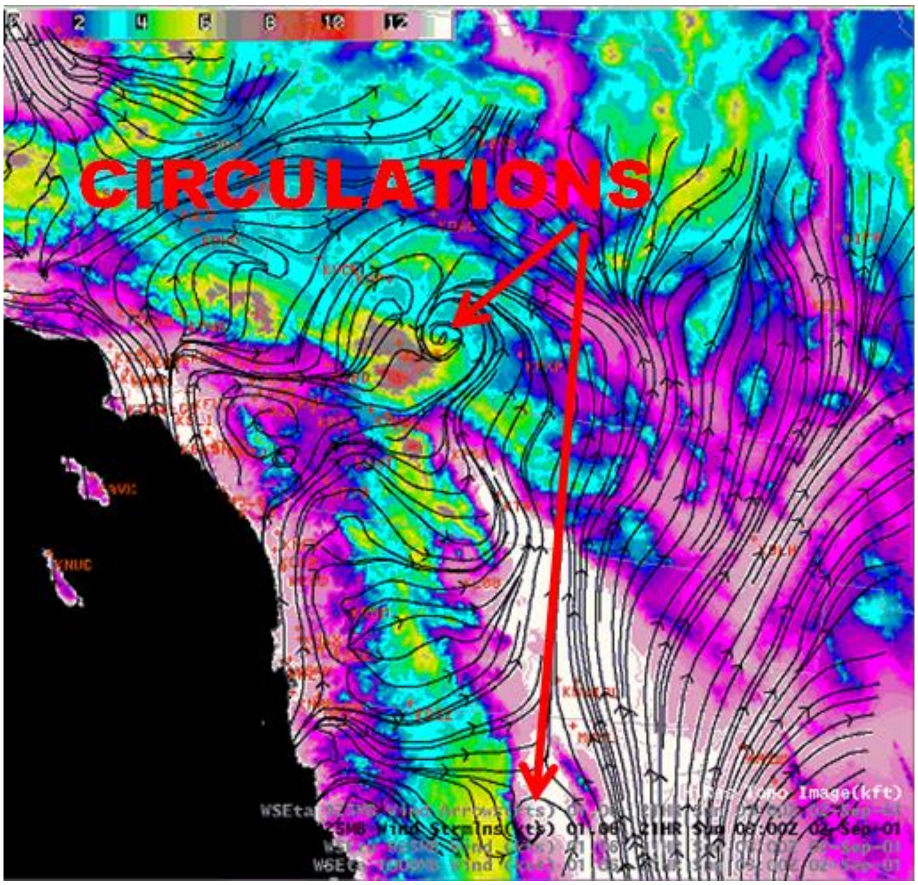

Fig. 5. The above imagery is the 925 mb streamlines overlaid on the Southern California terrain map from the 8 km Workstation ETA valid at 0800 UTC 2 September 2001. (Heights in the legend are in 1000’s of feet MSL)

4. CIRCULATIONS IN THE SAN BERNARDINO COUNTY MOUNTAINS/DESERTS

In figure 6 the circulations can be seen at higher resolution, thanks to the 3.7 km WRF-ARW run. Here the large circulations can be seen in the wind field and the velocity field (keying in on the Hesperia-to-Johnson Valley area in the center of the image).

The right panel is the satellite imagery, showing multiple circulations. There is a rather strong one on the backside of the mountains, and a weaker circulation north of it well into the deserts. (There is yet a third circulation noted to the southeast of the largest circulation). Forecasters can now take this into account in the forecast and warning process.

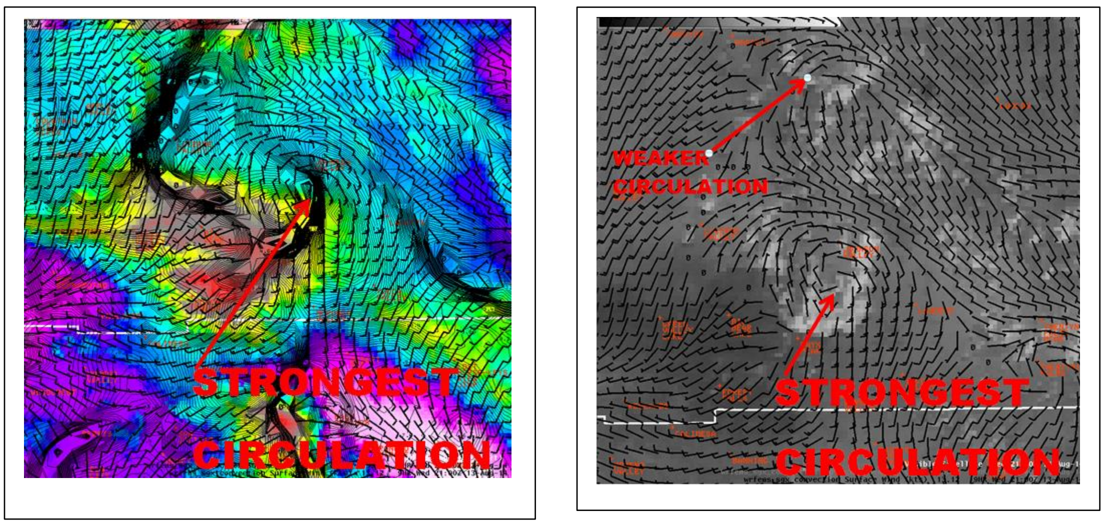

Fig. 6. The left image is the terrain map of Southern California centered on the San Bernardino County Mountains and adjacent deserts, (keying in on the Hesperia-to-Johnson Valley area in the center of the image). Included is the 9 hour 3.7 km WRF-EMS surface wind forecast (black barbs) and surface isotachs (contours) valid at 2100 UTC 13 August 2014. Convergent areas can be seen via the tight gradient in the isotachs. Depicted on the right is the 9 hour 3.7 km WRF-EMS surface wind forecast (black barbs) overlaid on the visible satellite imagery valid at 2100 UTC 13 August 2014.

5. CIRCULATIONS IN THE SAN DIEGO COUNTY MOUNTAINS/DESERTS

Figure 7 is satellite and surface wind imagery showing the early afternoon on one panel, and the late afternoon on the other panel. The left panel is showing convergence on the desert slopes of the San Diego County Mountains in the Warner Springs/ Borrego Springs/ Ocotillo Wells area. These images combine to show a good example of the evolution of two circulation centers. This is important, since it has been noticed that huge circulations have developed in the past in this area, with severe weather and flash flooding. This case shows how easily circulations can be seen at this even higher (1.5 km) resolution.

A common scenario is when there is southeasterly low level flow interacting with the westerly sea breeze or mountain/valley flows. The right panel shows a noticeable circulation pair in the cloud pattern as well as in the forecasted wind pattern. These circulations, along with a very moist and unstable air mass can enhance thunderstorm strength. These features pushing eastward, along with an approaching trough and/or with the "end of the day" sea breeze arrival, are good candidates to produce the final, and possibly the strongest storms of the day. This is especially true when the daytime convection shifts from the mountains to the deserts due to the sea breeze air stabilizing the mountain crests, and activation of the sea breeze/monsoon interface in the desert occurs.

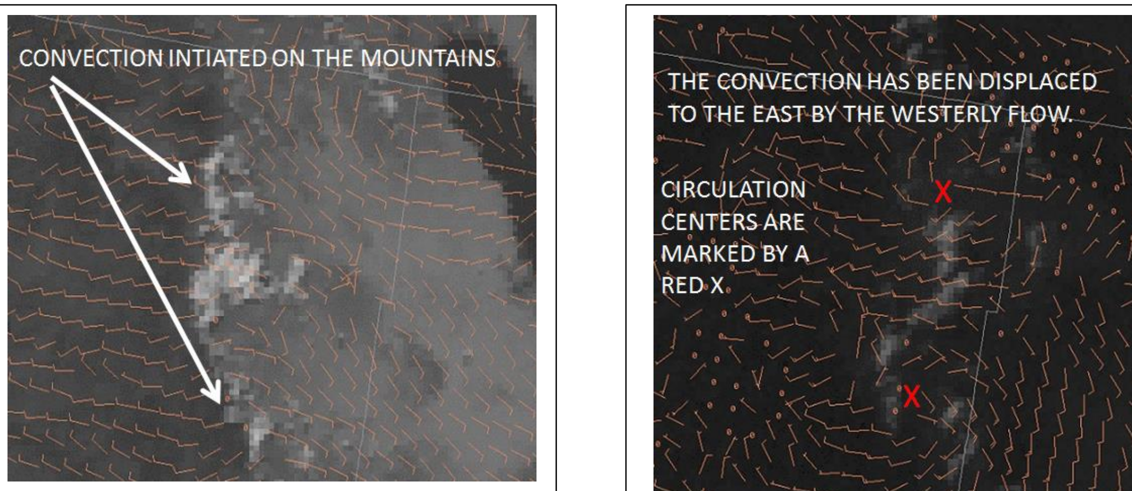

Fig. 7. The left panel is the 10 hour 1.5 km WRF-EMS ARW surface wind forecast valid at 2200 UTC 13 August 2014, overlaid on the 2200 UTC 13 August 2014 visible satellite imagery. The right panel is the 14 hour 1.5 km WRF-EMS ARW surface wind forecast valid at 0200 UTC 14 August 2014 overlaid on the 0200 UTC 14 August 2014 visible satellite imagery (image is dark since it is just before sundown).

6. RADAR IMAGERY OF CIRCULATIONS IN THE SAN DIEGO COUNTY MOUNTAINS AND DESERTS

Figure 8 is an example of what can occur under very moist and unstable conditions in the deserts, along with optimal flow conditions. The images [using GR2Analyst software (2013)] are looking northwest from the Yuma Radar (KYUX), located near the extreme southwestern corner of Arizona. The storm motion chosen was 360 degrees at 20 knots in order to make the circulations "stand out" better in the storm relative velocity.

At least 2 strong circulations can be seen over the eastern slopes of the San Diego County Mountains and in the deserts. Proximity to the mountains may be responsible for enhancing the circulations in the area via flows near the mountains (especially the large circulation on the far left). The circulations may drift to the east after forming near the mountains. These areas are prone to flash flooding and the development of severe thunderstorms. It is possible that these flows can help generate these severe thunderstorms and flash flooding events.

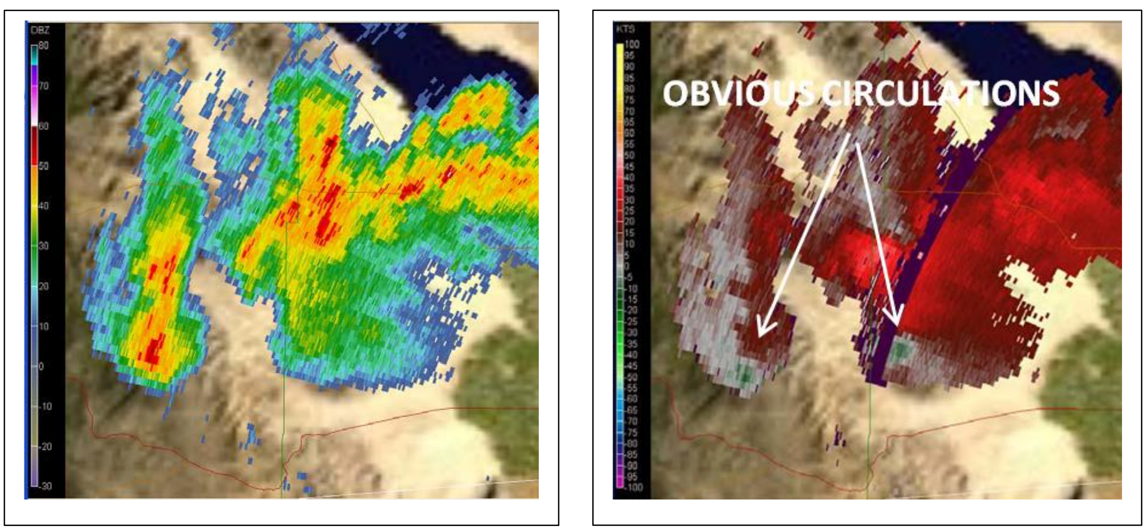

Fig. 8. The left panel is the 2324 UTC 13 July 2012 KYUX 1.4 degree base reflectivity and on the right is the 2324 UTC 13 July 2012 KYUX 1.4 degree storm relative velocity

7. MOUNTAIN WAVE CASE AT BURNS CANYON

Strong winds are a common occurrence in southern California. The most well-known are the Santa Ana winds (Jones et al., 2010). These are the generally hot, dry winds that blow from the desert to the sea. Lesser known are the onshore flow wind events (Small, 2006). During these events in Southern California, the wind generally blows from a south through northwest direction, and can produce downslope winds as strong as Santa Ana Wind events.

Wind gusts in excess of 45 m/s (approximately 100 mph) have been observed with both types of events. Similar to Santa Ana Winds, we can experience wind shear and mountain wave rotor activity. Erratic wind shifts during such events can be especially hazardous for aviation and firefighting operations. A good example of a strong onshore flow wind event occurred on 30 January 2014. On 30 January 2014 during strong onshore flow, a strong mountain wave and rotor hit Burns Canyon (BCNC1), gusting to over 80 mph (figs. 9 and 10).

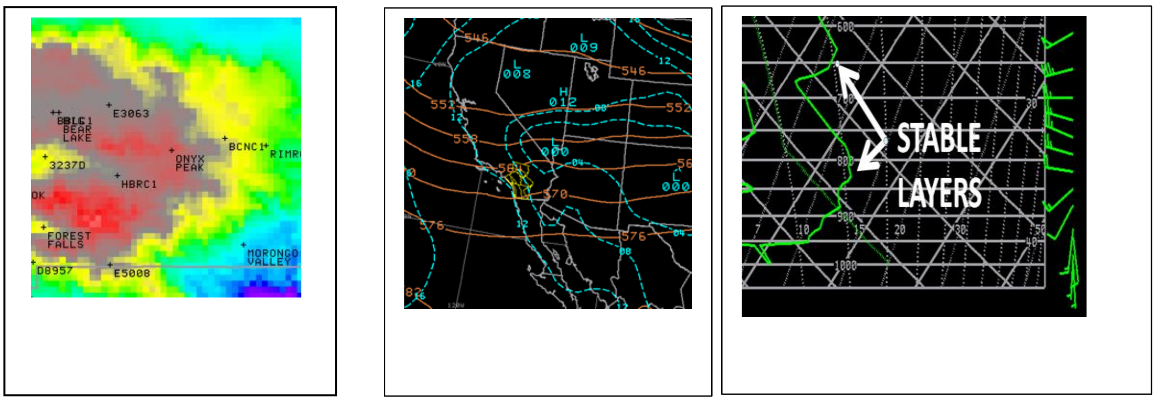

Fig. 9. The image on the left is a high resolution terrain map of Southern California showing the location of Burns Canyon (BCNC1). The middle image is the NAM80 500 mb height and mean sea level pressure for 0000 UTC 31 January 2014. On the right is the 1200 UTC 30 January 2014 KNKX sounding (just north of San Diego).

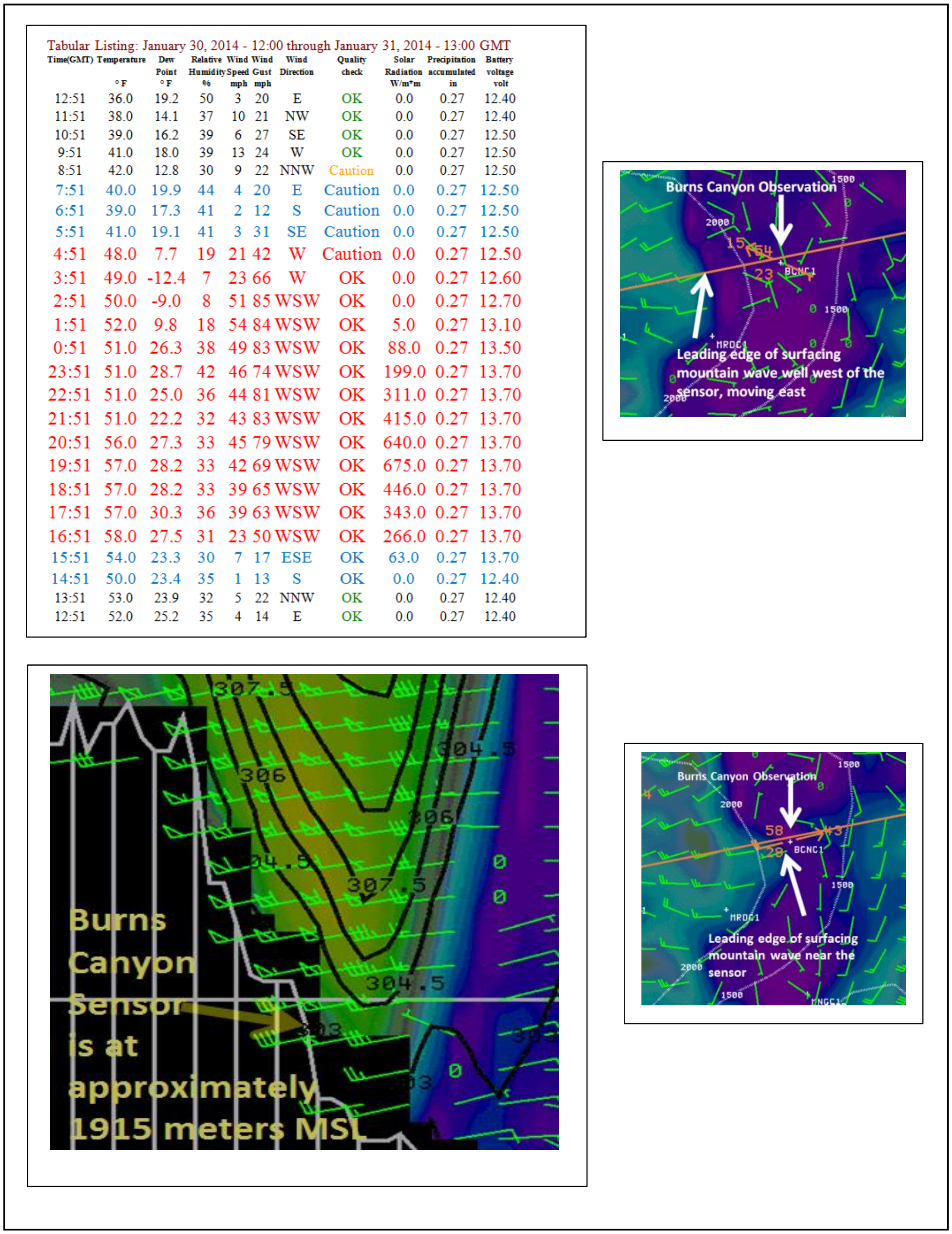

Tabular Listing: January 30, 2014 - 12:00 through January 31, 2014 - 13:00 GMT

Time(GMT)	Temperature °F	Dew Point °F	Relative Humidity %	Wind Speed mph	Wind Gust mph	Wind Direction	Quality check	Solar Radiation W/m*m	Precipitation accumulated in	Battery voltage volt
12:51	36.0	19.2	50	3	20	E	OK	0.0	0.27	12.40
11:51	38.0	14.1	37	10	21	NW	OK	0.0	0.27	12.40
10:51	39.0	16.2	39	6	27	SE	OK	0.0	0.27	12.50
9:51	41.0	18.0	39	13	24	W	OK	0.0	0.27	12.50
8:51	42.0	12.8	30	9	22	NNW	Caution	0.0	0.27	12.50
7:51	40.0	19.9	44	4	20	E	Caution	0.0	0.27	12.50
6:51	39.0	17.3	41	2	12	S	Caution	0.0	0.27	12.50
5:51	41.0	19.1	41	3	31	SE	Caution	0.0	0.27	12.50
4:51	48.0	7.7	19	21	42	W	Caution	0.0	0.27	12.50
3:51	49.0	-12.4	7	23	66	W	OK	0.0	0.27	12.60
2:51	50.0	-9.0	8	51	85	WSW	OK	0.0	0.27	12.70
1:51	52.0	9.8	18	54	84	WSW	OK	5.0	0.27	13.10
0:51	51.0	26.3	38	49	83	WSW	OK	88.0	0.27	13.50
23:51	51.0	28.7	42	46	74	WSW	OK	199.0	0.27	13.70
22:51	51.0	25.0	36	44	81	WSW	OK	311.0	0.27	13.70
21:51	51.0	22.2	32	43	83	WSW	OK	415.0	0.27	13.70
20:51	56.0	27.3	33	45	79	WSW	OK	640.0	0.27	13.70
19:51	57.0	28.2	33	42	69	WSW	OK	675.0	0.27	13.70
18:51	57.0	28.2	33	39	65	WSW	OK	446.0	0.27	13.70
17:51	57.0	30.3	36	39	63	WSW	OK	343.0	0.27	13.70
16:51	58.0	27.5	31	23	50	WSW	OK	266.0	0.27	13.70
15:51	54.0	23.3	30	7	17	ESE	OK	63.0	0.27	13.70
14:51	50.0	23.4	35	1	13	S	OK	0.0	0.27	12.40
13:51	53.0	23.9	32	5	22	NNW	OK	0.0	0.27	12.40
12:51	52.0	25.2	35	4	14	E	OK	0.0	0.27	12.40

Fig. 10. The upper left panel is a snapshot of the Mesowest observations for BCNC1. The local 1.5 km WRF-EMS ARW nest surface maps are the 4 hour forecast valid at 1600 UTC 30 January 2014 (upper right) and the 5 hour forecast valid at 1700 UTC 30 January 2014 (lower right) when the wave arrived. The images include wind barbs, wind speed (shaded) and model terrain (thin white lines, in meters MSL). The 10 hour forecast cross section valid at 2200 UTC 30 January 2014 (taken along the orange line) is shown in the lower left. The wind speed (shaded), the wind barbs (green, in knots), and the potential temperatures (black contours) are shown.

The 1200 UTC 30 January 2014 KNKX sounding shows a stable layer (inversion) near 5,000 feet MSL and 10,000 feet MSL, with moderate-strong westerly flow. The observations in fig. 10 show southeasterly rotor winds in blue text, which brackets the much stronger, westerly wind phase of the event (red text) during the peak of the windstorm. The model forecasted a wave surfacing very close to the sensor at 1700 UTC. (The wave and strong west winds arrived at 1700 UTC). So In this case, the surfacing strong west winds were still a bit west of Burns Canyon in the model when the winds actually surfaced. The 10 hour forecast indicated 40-50 knot sustained winds at Burns Canyon (fig. 10, lower left), similar to the 45-55 mph winds seen in the observation.

8. MOUNTAIN WAVE CASE AT BORREGO SPRINGS AND OCOTILLO WELLS

On 8 April 2013 a strong mountain wave in westerly flow brought damaging winds to the mountains and deserts of Southern California. The onshore pressure gradients peak in the spring and early summer, so it is not unusual for the synoptic pattern common for strong onshore winds to develop. Figure 11 shows a rapidly moving disturbance in the mountains and deserts. During this event, very strong 700 mb winds developed (fig. 12). The 3.7 km WRF was indicating numerous 70 kt or higher wind barbs on the desert slopes, even surpassing the 700 mb winds in some of those areas. There are some sustained winds of 75 to 80 kt extending from the coastal slopes out into the deserts in the model.

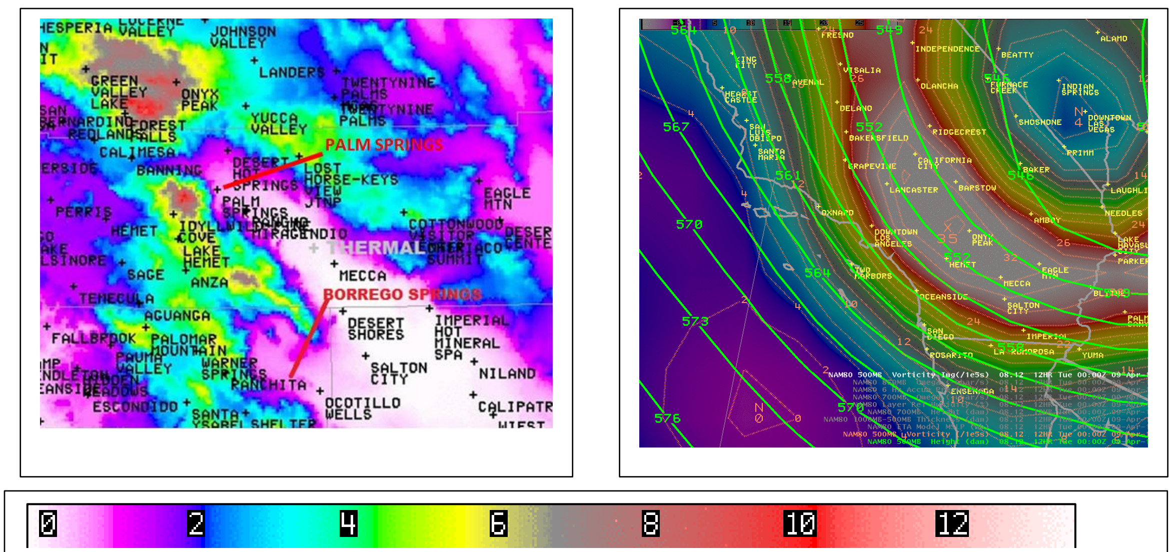

Fig. 11. The left panel is the terrain map for Southern California with the locations of Palms Springs and Borrego Springs indicated. The image on the right is the 12 hour forecast, NAM80 500 MB heights (contours) and vorticity (dashed, shaded) valid at 0000 UTC 9 April 2013.

The Palm Springs-Borrego Valley-Ocotillo Wells area was especially hard hit.

One spotter report indicated the following in the Ocotillo Wells area:

“Trees down and damage to buildings, brown outs due to total power outage as of 938 AM (1638 UTC) was reported from residents…Highest gust reported in area was 73 mph. [At 920 AM (1620 UTC) the Ocotillo Wells mesonet reported a gust to 73 mph].”

Another spotter report follows:

“At 1236 PM (1936 UTC), Power is out all over Borrego Springs. Major power line into town is down from earlier gusts of 83+ mph. Lots of branches down around town as well…with at least one road blocked. Current winds…west 30 to 35 mph…with gusts to 56 mph.”The Ocotillo Wells wind observations are in figure 13.

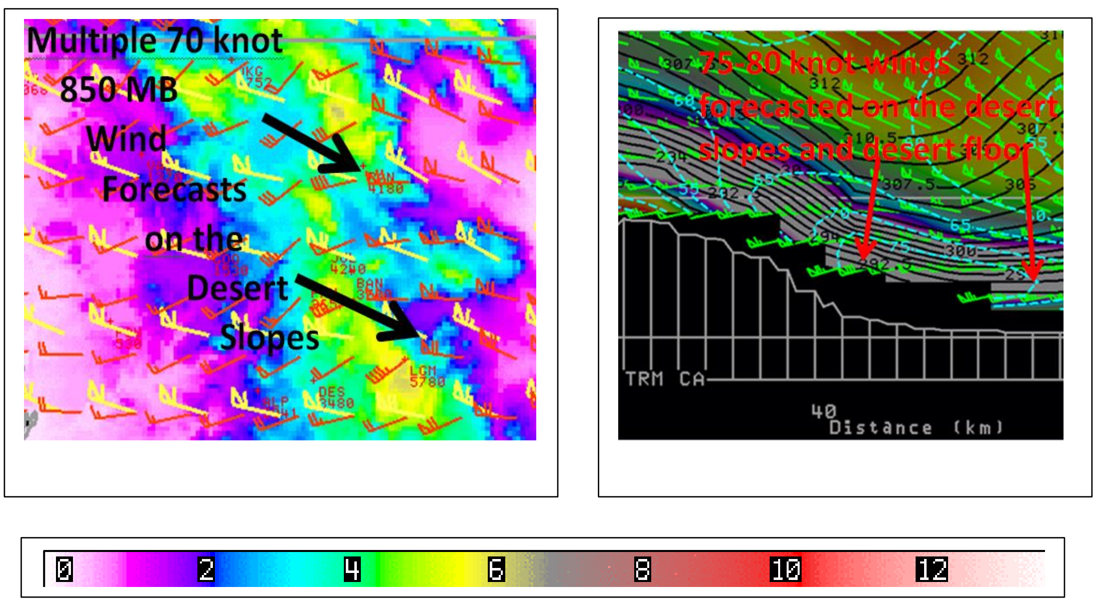

Fig. 12. The left panel is the 6 hour 3.7 km WRF-EMS winds valid at 1800 UTC 8 April 2013. The 700 MB (yellow wind barbs) and 850 MB (red wind barbs) are shown. The right image is the 6 hour 3.7 km WRF-EMS cross section valid at 1800 UTC 8 April 2013. The winds are the green wind barbs, the isotachs are in cyan, and the black lines are the potential temperature. The shading is the temperature lapse rate.

DATE/TIME	TEMP	RH	WIND SPEED	WIND GUST	GUST DIRECTION
4-8-2013 15:15 GMT	64	52	29	60	246
4-8-2013 15:18 GMT	64	52	29	60	246
4-8-2013 15:21 GMT	65	52	23	44	240
4-8-2013 15:30 GMT	65	49	28	60	255
4-8-2013 15:35 GMT	65	50	28	53	274
4-8-2013 15:40 GMT	64	51	32	61	252
4-8-2013 15:45 GMT	65	50	32	57	262
4-8-2013 15:50 GMT	65	50	35	67	242
4-8-2013 15:55 GMT	64	49	31	56	228
4-8-2013 16:00 GMT	65	49	33	57	218
4-8-2013 16:05 GMT	65	49	36	68.9	262
4-8-2013 16:08 GMT	65	49	36	68.9	262
4-8-2013 16:15 GMT	64	50	34	62.9	269
4-8-2013 16:20 GMT	64	51	36	72.9	245
4-8-2013 16:30 GMT	65	47	39	64.9	252
4-8-2013 16:35 GMT	65	47	39	64.9	252
4-8-2013 16:40 GMT	65	48	35	67	229
4-8-2013 17:00 GMT	66	42	30	53	238
4-8-2013 17:05 GMT	66	46	24	49	245
4-8-2013 17:10 GMT	67	39	29	51	233
4-8-2013 17:15 GMT	66	43	25	50	260
4-8-2013 17:30 GMT	68	37	16	40	271
4-8-2013 17:35 GMT	67	42	18	46	284
4-8-2013 17:40 GMT	67	41	19	39	266
4-8-2013 17:43 GMT	67	41	19	39	266
4-8-2013 17:48 GMT	66	44	27	60	276
4-8-2013 17:50 GMT	66	44	27	60	276
4-8-2013 18:00 GMT	66	47	22	55	266
4-8-2013 18:15 GMT	65	48	27	57	248
4-8-2013 18:17 GMT	65	48	27	57	248

Fig. 13. The above data is a snapshot of the Mesowest observations for Ocotillo Wells [KD6RSQ-5 Ocotillo Wells, CA (AS938)]. The winds peaked at about 35-40 mph with gusts to around 70-75 mph, somewhat lower than the model wind forecasts.

Sustained winds in the model were significantly higher than what was being reported there, and actually the model-forecasted sustained winds were even a bit higher than the wind gusts there (a straight comparison is being done here, with no consideration of model wind heights and sensor or spotter report heights). As seen in previous local studies (and also in Fovell, 2012, as well as in Fovell and Cao, 2013), there is an inverse relationship between the ratio of the reported wind gusts for offshore (Santa Ana Winds) and the model sustained winds at some locations. Basically, the gust factor (or “gust ratio”) decreases for increasing model wind speeds for some sites for the stronger events. This also seems to be the case for onshore flow wind events as well. The reduction in the ratio seems to be especially noticeable for extreme events such as this one, and ratios may be very close to a value of 1 for some types of events in some areas based on the reliable, currently available data in this region, (possibly where very strong onshore winds occur and/or are forecast by the model). The Palm Spring/Borrego Springs/Ocotillo Wells area spotter reports and 3.7 km WRF sustained surface winds may be an example of such a case. More investigation will be conducted to look at this.

9. SUMMARY AND CONCLUSIONS

The 1.5 km resolution data, (in addition to the 3.7 km and much earlier 8 km local model runs) has progressively allowed us to take a closer look at several local phenomena and implement the findings operationally (Special thanks to Brian D’Agostino and Steven Vanderburg for their support on this project). We see that it can accurately forecast the sea breeze (at least in this case) in the Palm Springs area. For the Burns Canyon mountain wave case, it captured the rotor flow at Burns Canyon and was close on the timing of the surfacing wave. Overall, the models seem to be better with the timing and intensity (including whether or not the strong winds occur) at the typically windier sites when the sensor is well inside a corridor of strong winds in the model, (rather than when the site is near the edge of the corridor of strong winds). This applies to both onshore and offshore flow events.

The model seems to have a good idea on the locations of convergence boundaries. We can now have more confidence in the model wind patterns for timing and intensity, from mountain waves to sea breezes, as well as for convergence zones, convective initiation, and strength.

10. REFERENCES

Fovell, R. G., 2012: Downslope windstorms of San Diego County: Sensitivity to resolution and model physics. 13th WRF Users Workshop, Boulder, CO, Nat. Center for Atmos. Res. https://www.regonline.com/AttendeeDocuments/1077122/43389114/43389114_1045166.pdf

Fovell, R. G., and Y. Cao, 2013: Predictability and sensitivity of downslope windstorms in San Diego County. 15th Conference on Mesoscale Processes, Portland, OR, https://ams.confex.com/ams/15MESO/webprogram/Manuscript/Paper228055/cao_fovell_meso_paper.pdf

Gibson Ridge Software, 2013: GRlevel2Analyst Version, 2.0. [Available online at http://www.grlevelx.com/.]

Jones, C., F. Fujioka, and L.M.V. Carvalho., 2010. Forecast Skill of Synoptic Conditions Associated with Santa Ana Winds in Southern California. *Mon. Wea. Rev.,* 138, 4528-4541. http://journals.ametsoc.org/doi/abs/10.1175/2010MWR3406.1

Small, I. J., T. Mackechnie, and B. Bower, 2000: Mesoscale Interactions Triggering Severe Thunderstorms and Flash Flooding in Southwestern California - July 1999. Western Regional Technical Attachment 00-01. http://www.wrh.noaa.gov/media/wrh/online_publications/TAs/ta0001.pdf

Small, I. J., 2006: Forecaster's Handbook for Extreme Southwestern California Based On Short Term Climatological Approximations: Part II – Wind Effects on Terrestrial and Marine Environments. NOAA Technical Memorandum NWS WR-278 http://www.wrh.noaa.gov/wrh/techMemos/TM-278.pdf